

Depairing field, onset temperature and the nature of the transition in cuprates

Lu Li¹, Yayu Wang¹, J. G. Checkelsky¹, M. J. Naughton²,

Seiki Komiya³, Shimpei Ono³, Yoichi Ando³ and N. P. Ong^{1*}

¹Department of Physics, Princeton University, Princeton, NJ 08544

²Department of Physics, Boston College, Chestnut Hill, Massachusetts 02467, U.S.A

³Central Research Institute of Electric Power Industry, Komae, Tokyo 201-8511, Japan

(Dated: February 6, 2008)

The depairing (upper critical) field H_{c2} in hole-doped cuprates has been inferred from magnetization curves $M-H$ measured by torque magnetometry in fields H up to 45 T. We discuss the implications of the results for the pair binding energy, the Nernst onset temperature, fluctuations and the nature of the Meissner transition at T_c .

PACS numbers: 74.25.Dw, 74.72.Hs, 74.25.Ha

In hole-doped cuprates, the depairing field at which the pair condensate is destroyed (or “upper critical field” H_{c2}) has been notoriously difficult to measure. Recently, progress has been achieved using the vortex-Nernst effect [1, 2, 3] and high-field torque magnetometry [4, 5].

High-field measurements of M are technically difficult because the large Ginzburg-Landau parameter, small crystal volumes (0.1-0.3 mm³) and high field scales of H_{c2} (50-200 T) all result in a very small sample moment. Fortunately, torque magnetometry is well-suited for this purpose [6]. The crystal is glued to the end of a soft cantilever with its axis \mathbf{c} at a small angle to \mathbf{H} . The observed magnetization $M_{eff} = \Delta\chi H_z + M(T, H_z)$, where $M(T, H_z) < 0$ is the magnetization produced by supercurrents ($\hat{\mathbf{z}}||\mathbf{c}$ and T is the temperature). The dominant contribution to the paramagnetic background $\Delta\chi$ comes from the strongly anisotropic orbital (van Vleck) term χ_i^{orb} . Its weak T -linear behavior allows the diamagnetic term M to be extracted with high resolution [5]. Here we discuss some of our torque measurements on La_{2-x}Sr_xCuO₄ (LSCO), Bi₂Sr_{2-y}La_yCuO₆ (Bi 2201) and Bi₂Sr₂CaCu₂O₈ (Bi 2212) from the underdoped (UD) to overdoped (OD) regimes.

Figure 1 shows the $M-H$ curves in optimally-doped (OP) Bi 2212 ($T_c \sim 86.5$ K) at temperatures 35 to 90 K (left panel), and from 80 to 110 K (right panel). The curves are all fully reversible (pinning effects appear only below 35 K at low fields < 1 T). At the lowest T , the curve of M vs. H is very similar to that in a low- T_c type II superconductor. Above H_{c1} , $|M|$ decreases as $\log H$ over a very broad field range. A notable feature is the very high H_{c2} , which we estimate to be 150-200 T by extrapolation. (These values are much larger than inferred from measurements of the resistivity ρ vs. H . The “knee” feature in ρ usually used to fix “ H_{c2} ” actually occurs just above the vortex-solid melting field $H_m \ll H_{c2}$.)

As T nears T_c , a major difference from BCS superconductors emerges. There, $H_{c2}(T)$ decreases to zero lin-

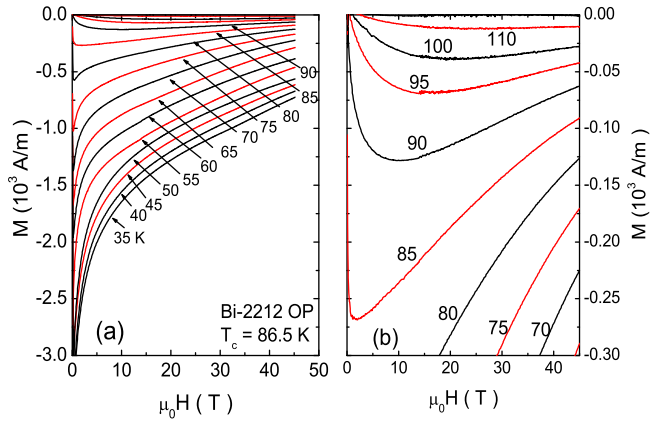


FIG. 1: Magnetization curves M vs. H in OP Bi 2212 at $T = 35-90$ K (Panel a) and at $T = 75-110$ K (b). At low T , $|M| \sim \log H$ initially, but goes to zero at $H_{c2} = 150-200$ T. Notably, $H_{c2}(T)$ shows no tendency towards zero as $T \rightarrow T_c^-$. Above T_c (86.5 K), $|M|$ remains quite large in fields up to and above 45 T.

early, viz. $H_{c2}(T) \sim t$ with $t = 1 - T/T_c$. Accordingly, the high-field limit of M in Fig. 1b should decrease and reach zero at T_c . Instead, we find that it remains high above our maximum field (45 T), even when T exceeds T_c (right panel). The diamagnetic signal remains quite large at 45 T up to 110 K.

This key feature – seen in all the hole-doped cuprates studied – is most apparent in single-layer UD Bi 2201, where complete suppression of diamagnetism is attainable below 45 T. Figure 2 shows the $M-H$ curves in a crystal with $T_c \sim 14$ K. Hysteretic behavior is not observed down to 4 K. In comparison with OP Bi 2212, the magnitude $|M|$ in weak H and low T is quite a bit smaller (250 A/m compared with 4000 A/m), but it displays the same $\log H$ dependence in $H < 20$ T. At high fields, M approaches zero at the field $H_{c2}(0) \sim 43$ T. In Panel b, we show that $H_{c2}(T)$ remains nominally T -independent even above T_c . In the interval around T_c , the $M-H$ curves display the same pattern as shown for OP Bi 2212. Significant diamagnetism remains at T up to 30 K.

*Proceedings M²S-HTSC-VIII, Dresden 2006, Physica, in press.

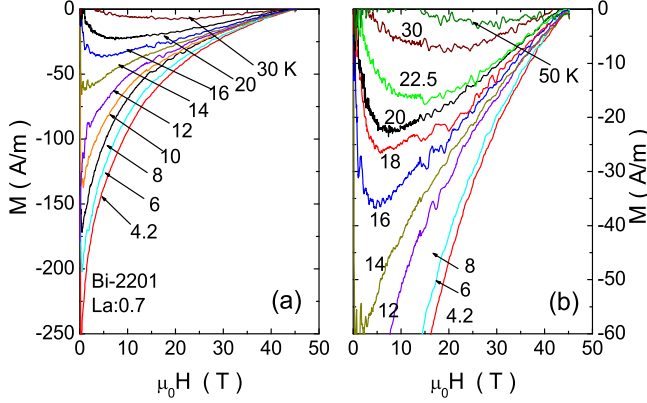


FIG. 2: Magnetization curves M vs. H in UD Bi 2201 shown for $T = 4.2\text{--}30$ K (Panel a), and in expanded scale (Panel b). At each T , the field at which $|M| \rightarrow 0$ is taken to be $H_{c2}(T)$. The convergence of all curves implies that $H_{c2(T)}$ is independent of T to our resolution. Above $T_c \sim 14$ K, M remains sizeable and strongly H dependent.

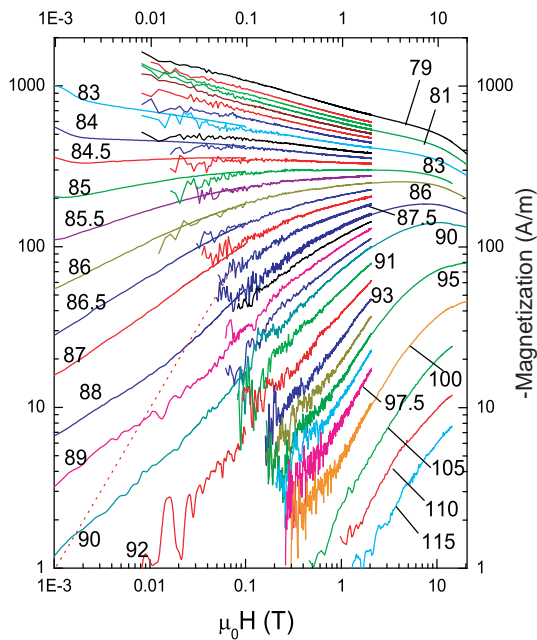


FIG. 3: The field dependence of $M(T, H)$ in OP Bi 2212 from $H = 10$ Oe to 20 T at $T = 79\text{--}115$ K. The log-log plot shows that, as $H \rightarrow 0$, $M(H)$ follows the fractional power-law $M \sim H^{1/\delta}$. The plot combines SQUID results (10 to 1000 Oe) and torque magnetometry results (500 Oe to 2 T). Torque results up to 20 T are also shown at selected T . Linear response $M \sim H$ at 87 K would appear as the dashed line (from Ref. [4]).

The diamagnetic signal M above T_c is robust to fields of 45 T and considerably larger in magnitude than “fluctuating diamagnetism” in low- T_c superconductors [9]. We discuss why the fluctuations are distinctly non-Gaussian. In BCS superconductors, a key feature is the linear decrease to zero of the T -dependent critical field

$H_{c2}(T)$ as $T \rightarrow T_c^-$. This feature dictates the behavior of fluctuations above T_c in Gaussian GL treatments. In particular, t enters in $M(t, h)$ as the ratio $|t|/h$. Consequently, above T_c , the field dependence of M is dictated by the field scale $H_{c2}(0)t$, which is the “mirror image” of $H_{c2}(T)$, vanishing linearly in $|t|$ as $T \rightarrow T_c$ from above. Accordingly, M measured in low- T_c superconductors are nicely scaled when plotted in terms of the “Prange” variable $x = [\frac{dH_{c2}}{dT}]_c(T - T_c)/H \sim 1.4|t|/h$ [9].

As noted above, $H_{c2}(T)$ does not vanish linearly in $|t|$ in hole-doped cuprates [3, 4, 5]. This invalidates the Gaussian approach which depends on series expansion in terms of the order parameter and its derivative. Above T_c , the M - H curves in Bi 2212 are also qualitatively different from low- T_c superconductors. Instead of linear response, the M - H curves are strongly nonlinear even in low H . Figure 3 shows in log-log scale the variation of M over a broad range of H (10 G to 30 T) at $T = 79\text{--}115$ K. As emphasized in Fig. 4a, the M - H curves display strong curvature at temperatures near $T_c = 87$ K. In weak H , $M(H)$ fits well to the power law

$$|M| \sim H^{1/\delta}, \quad (1)$$

with a strongly T dependent exponent $\delta(T)$. Between T_c and 105 K, $\delta(T)$ decreases from ~ 10 to 1 (Fig. 4b). The vanishing of $\delta(T)$ defines the temperature T_s slightly below T_c at which M is *independent* of H up to a few T (this feature – dubbed the separatrix [4] – has been known for a long time).

These anomalous magnetization patterns are incompatible with Gaussian fluctuations, but consistent with the phase-disordering scenario [7] in which, above T_c , the condensate amplitude is large, but phase rigidity and long-range phase coherence are lost. Near T_c , the M - H curves are strikingly similar to those calculated for a 2D superconductor near its Kosterlitz Thouless (KT) transition [8]. As discussed later, the appropriate comparison is with the 3DXY model with very large anisotropy.

The M - H curves in Figs. 1-3 together imply the following physical picture (see Ref. [4]). On cooling from 300 K, the system first crosses the pseudogap temperature T^* . The pseudogap affects primarily the spin degrees of freedom, especially the relaxation rate $1/T_1T$ in NMR and the bulk susceptibility. Evidence for Cooper charge pairing appears only at $T_{onset} = 0.5\text{--}0.7 T^*$. Below T_{onset} (the “Nernst” region), both the Nernst signal and diamagnetism increase steeply to merge smoothly with the corresponding signals below T_c . Within each CuO_2 layer, the pair condensate is robust with a very large pair-binding energy. However, because of thermal generation of mobile 2D vortices, phase coherence is confined to a length scale given by the phase correlation length ξ_ϕ [4]. The “hot 2D vortex liquid”, nonetheless, displays a fairly large diamagnetic response.

It is instructive to contrast cuprates from a percolative system (e.g. granular Al) in which superconducting islands are gradually phase coupled by the proximity effect as T decreases. In high-quality crystals of the cuprates,

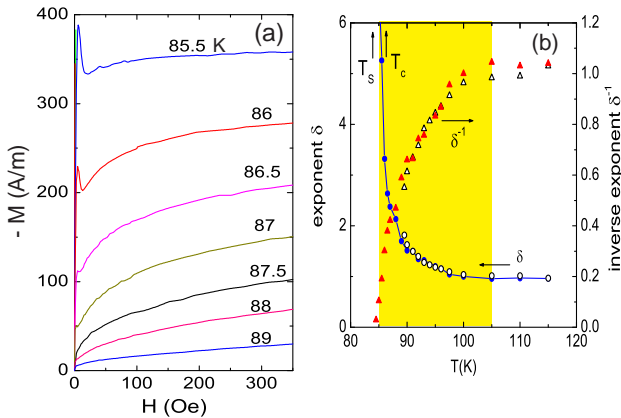


FIG. 4: (Panel a) The weak-field M - H curves near T_c ($= 87$ K) in OP Bi 2212. The power-law variation with fractional exponent is evident in all curves shown. Below T_c , full flux expulsion occurs for $H < H_{c1}$ (visible as a spike). The curve at 85.5 K is very close to the separatrix temperature T_s . Panel (b) displays the T dependence of the exponent $\delta(T)$ (circles) for 2 crystals of OP Bi 2212. The reciprocal $\delta(T)^{-1}$ is plotted as solid and open triangles for the 2 samples. As $T \rightarrow T_s^+$, $\delta(T)^{-1}$ decreases smoothly to 0. In the shaded region where $\delta > 1$ (from T_s to 105 K), linear magnetic response is absent even at 10 Oe (adapted from Ref. [4]).

the zero-field transition is invariably very sharp. At T_c , full flux expulsion appears [4]. The resistive transition is also abrupt, in contrast to the long tail seen in granular Al.

Two features seem to be crucial. The first is the pre-emption of the 2D KT transition in individual layers by the 3D transition caused by interlayer coupling, as occurs in layered magnets [10]. Below $T_{onset} \sim 130$ K, the in-plane ξ_ϕ (inferred from the susceptibility $\chi = M/H$) grows as in the KT transition [4]. Below 105 K, however, M becomes increasingly non-linear (Fig. 4a). The increase in $\delta(T)$ reflects rapid upward renormalization of the interlayer coupling strength. In the interval between T_c and 105 K, the fractional power-law implies that χ can approach -1 in the limit $H \rightarrow 0$. However, this London rigidity is fragile and easily suppressed by field. At T_c (~ 2 K above T_s), the Meissner state appears [4]. As apparent in Fig. 4a, full flux expulsion occurs below the lower critical field $H_{c1}(T)$, seen as sharp spikes in Fig. 4a. Significantly, the 3D Meissner state is observed at fields $H < H_{c1}$, yet at higher H ($>$ a few T), the M - H profiles revert to the 2D pattern seen high above T_c . This field-induced crossover from 3D to 2D behavior – with its intrinsic non-monotonicity – is very different from low- T_c superconductors.

The second feature is the termination of the melting curve $H_m(T)$ at T_c . Far from being accidental, we believe this is intrinsic to the nature of the transition. Within the vortex-solid state, spontaneously created vortices are ineffectual in destroying phase coherence because they are not able to diffuse. Hence, T_c cannot lie below the

high- T termination of $H_m(T)$. On the other hand, T_c cannot lie above the termination point. This would correspond to a strictly 2D transition that is incompatible with the observed full Meissner effect. These 2 features distinguish the cuprate transition from that in granular Al.

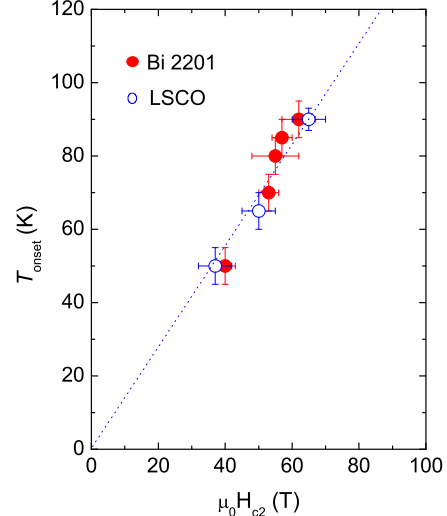


FIG. 5: Plot of T_{onset} vs. $H_{c2}(0)$ in the single-layer cuprates Bi 2201 and LSCO. Both quantities are inferred from the M vs. H curves measured by high-field torque magnetometry. The broken line is Eq. 2 with $g \simeq 2.1$.

Lastly, we discuss an interesting relation between H_{c2} and T_{onset} . Measurements on several Bi 2201 and LSCO crystals from UD to OD regime reveal that $H_{c2}(0)$ and T_{onset} (measured from both the Nernst signal and magnetization) scale together as shown in Fig. 5. Within the experimental uncertainties, T_{onset} is linear in $H_{c2}(0)$. Expressing $H_{c2}(0)$ as a Zeeman energy, viz.

$$k_B T_{onset} = g \mu_B H_{c2}(0), \quad (2)$$

we find that the g-factor $g \simeq 2.1$ (μ_B is the Bohr magneton). The data in Fig. 5 are restricted to Bi 2201 and LSCO. As noted in Fig. 1, $H_{c2}(0)$ in OP Bi 2212 is much larger given its T_{onset} (~ 130 K). Figure 5 ties together the energy scale implied by T_{onset} and the pair binding energy at low T for Bi 2201 and LSCO. The linear fit with $g \sim 2.1$ suggests that the Pauli limit may be relevant to the high-field depairing process. The implication of this relationship is currently being explored.

We acknowledge discussions with P. W. Anderson, S. A. Kivelson, Z. Tesanovic, V. Oganesyan, S. Sondhi, D. A. Huse and Z. Y. Weng. Measurements were performed at the National High Magnetic Field Laboratory, Tallahassee, which is supported by the U.S. National Science Foundation (NSF DMR-0084173), the State of Florida

and DOE. This research is supported by NSF Grant DMR 0213706.

- [1] Yayu Wang, Z. A. Xu, T. Kakeshita *et al.*, Phys. Rev. B **64**, 224519 (2001).
- [2] Yayu Wang, S. Ono, Y. Onose *et al.*, Science **299**, 86 (2003).
- [3] Yayu Wang, Lu Li, and N. P. Ong, Phys. Rev. B **73**, 024510 (2006).
- [4] Lu Li, Yayu Wang, M. J. Naughton *et al.*, Europhys. Lett., **72**, 451 (2005).
- [5] Yayu Wang, Lu Li, M. J. Naughton *et al.*, Phys. Rev. Lett., **95**, 247002 (2005).
- [6] C. Bergemann *et al.*, Phys. Rev. B **57**, 14387 (1998).
- [7] V. J. Emery and S. A. Kivelson, Nature **374**, 434 (1995); G. Baskaran, Z. Zou and P. W. Anderson, Solid State Commun. **63**, 973 (1987); S. Doniach and M. Inui, Phys. Rev. B **41**, 6668 (1990).
- [8] Vadim Oganesyan, David A. Huse and S. L. Sondhi, Phys. Rev. B **73**, 094503 (2006).
- [9] J. P. Gollub, M. R. Beasley, R. Callarotti, and M. Tinkham, Phys. Rev. B **6**, 3039 (1973).
- [10] K. Hirakawa and K. Ubukoshi, Jnl. Phys. Soc. Jpn. **50** 1909 (1981).